Selective Wrapping and Supramolecular Structures of Polyfluorene−Carbon Nanotube Hybrids

Jia Gao,[†] Maria Antonietta Loi,[†,*] Elton José Figueiredo de Carvalho,[‡] and Maria Cristina dos Santos[‡,*]

[†]Zernike Institute for Advanced Materials, University of Groningen, Nijenborgh 4, 9747 AG Groningen, The Netherlands, and [‡]Instituto de Física, Universidade de São Paulo, 05508-090 São Paulo SP, Brazil

Single walled carbon nanotubes (SWNTs) are long sp[2] carbon cylinders, often closed at the ends by some type of fullerene structure. The electronic structure of these systems depends on how the network of C−C bonds distributes along the cylinder axis. Formally, the classification of structures is made in terms of two integers (*n*,*m*), the so-called chiral indices, by which the tube diameter, perimeter, chiral angle, and ultimately the electronic properties are determined.[1] The chiral angle and diameter are given by $\tan \theta = \sqrt{3}m/(2n + m)$ and $d = (a_0/\pi)(n^2 + m^2 + nm)^{1/2}$, respectively, where a_0 is the length of the graphene primitive vectors. The electronic structure can be deduced from the chiral indices by a simple relation: nanotubes possessing chiral indices satisfying $(n - m) = 3q$ (*q* integer) are metallic or semimetallic while all the others are semiconducting. SWNT samples are formed by bundles containing tubules of the various chiralities, diameters, and electronic structures. The effective use of these systems in nanotechnology requires the availability of monodisperse samples, which led in recent years to the development of several separation techniques.[2] In one of these techniques, SWNTs are dispersed in toluene solutions of the conjugated polymer poly[9,9-dioctylfluorenyl-2,7-diyl](PFO). This polymer selectively wraps on certain nanotubes which are separated from the bundles. The fluorescence of the isolated, polymer-wrapped nanotubes suspended in the solutions can be observed.[3,4] The PFO selectivity privileges semiconducting nanotubes, a feature that has recently been used to prepare electronic devices on extended surface areas.[5] Among SWNT samples prepared by the high-pressure carbon monoxide

ABSTRACT We report on the photophysical properties of single-walled carbon nanotube (SWNT) suspensions in toluene solutions of poly[9,9-dioctylfluorenyl-2,7-diyl](PFO). Steady-state and time-resolved photoluminescence spectroscopy in the near-infrared and visible spectral regions are used to study the interaction of the dispersed SWNTs with the wrapped polymer. Molecular dynamics simulations of the PFO-SWNT hybrids in toluene were carried out to evaluate the energetics of different wrapping geometries. The simulated fluorescence spectra in the visible region were obtained by the quantum chemical ZINDO−CI method, using a sampling of structures obtained from the dynamics trajectories. The tested schemes consider polymer chains aligned along the nanotube axis, where chirality has a minimal effect, or forming helical structures, where a preference for high chiral angles is evidenced. Moreover, toluene affects the polymer structure favoring the helical conformation. Simulations show that the most stable hybrid system is the PFO-wrapped (8,6) nanotube, in agreement with the experimentally observed selectivity.

KEYWORDS: molecular dynamics · carbon nanotube wrapping · polyfluorene · photoluminescence

(HiPCO) method, the most commonly observed nanotubes through PFO wrapping are, in order of decreasing concentration, (8,6), (9,7), (8,7), (7,5). and (7,6). All these SWNTs have high chiral angles. Moreover, the selectivity depends strongly on the solvent used and on the nature of the side chain attached to the fluorene unit:[6,7] (i) in solutions of the solvent tetrahydrofuran the PFO selectivity is lost; (ii) changing the lateral alkyl chain of the polymer from octyl to hexyl increases the number of SWNT species selected and the chirality selectivity is lost; (iii) adding polar lateral chains like dimethylaminopropyl or the water-soluble trimethylammonium-propyl bromide to the fluorene unit also broadens the number of selected SWNTs. Selectivity hence appears to be related to the structural properties of the PFO−toluene system.

The structure of PFO chains in several solvents and in the solid state, as well as
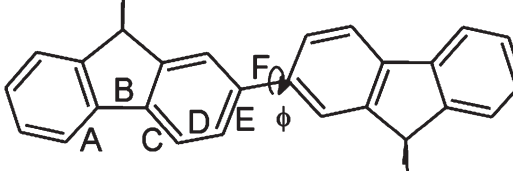
the way the structure affects the photophysical properties of this highly fluorescent polymer, have been a subject of continued interest in the literature.[8−10] Recent neutron diffraction studies combined to nuclear magnetic resonance and quantum chemical calculations[10] revealed that at low concentrations of PFO in toluene the chains are mainly isolated. Aggregation phenomena start to occur at low PFO concentrations and are increasingly important as concentration increases due to interpenetration of the polymer chains. The driving force to aggregation is the van der Waals interaction between the octyl lateral tails that interconnect the polymer chains like a zipper. The stabilization of the so-called β-phase is known to be dependent on the size of the lateral chain, being optimum for octyl. Smaller side chains have to compete with backbone−backbone interactions while longer side chains can bend and are more subjected to disorder effects. This partially ordered polymer phase is also dependent on the average polymer size since high molecular weight chains can fold and the aggregation induced by the lipid−lipid interaction of side chains from different portions of the same polymer backbone can occur.

Here we report on studies of PFO selectivity for high chiral angle SWNTs in toluene by steady-state and time-resolved photoluminescence spectroscopy in the near-infrared and visible spectral regions. We also carried out atomistic molecular dynamics simulations of these systems. We used conformations from the dynamics trajectories to calculate the emission spectrum of the polymer chains wrapping around the tubules and configuration averaged to compare the emission properties from different wrapping schemes. We conclude that the mechanism responsible for the selectivity is the same found for the stabilization of the β-phase. The alkyl tails of neighboring polymer chains zip and align, through van der Waals interactions, on similar zigzag motifs on the nanotube wall. The best coverage of the nanotube wall is obtained when the zipped polymer chains adopt a helical conformation, maximizing at the same time the $\pi-\pi$ interactions between nanotube and fluorene units and the network of octyl−octyl tails and the zigzag bonds on the nanotube wall. The geometry that maximizes these attractive interactions for PFO was calculated to be the (8,6) nanotube, in agreement with experiment. The observed modifications in the wrapped-polymer luminescence as compared to the polymer in solution give indications about the supramolecular arrangements of the PFO−SWNT system.

RESULTS AND DISCUSSION

To obtain the simulated fluorescence spectra and study how different wrapping geometries affect them, we devised a technique that uses a combination of classical molecular dynamics and quantum chemistry.

Scheme 1. Ground (GS) and excited (ES) state geometrical data for bifluorene as obtained from B3LYP and CIS calculations, respectively. FF data are for the optimized molecule in the modified CVFF force field. The labels A−F refer to bond lengths (Å) and ϕ to the torsion angle (degrees). Also indicated is λ_{max}(nm), obtained via the ZINDO/S−CI method.

	A	B	C	D	E	F	ϕ	λ_{max}
GS	1.397	1.467	1.396	1.394	1.408	1.484	37.9	334.6
ES	1.400	1.434	1.408	1.362	1.440	1.423	9.8	382.7
FF	1.428	1.433	1.414	1.397	1.440	1.413	32.1	378.1

For this purpose, adjustments in the force field (FF) parameters were made, as described in the Methods section, to obtain a PFO equilibrium conformation closer to that of the excited state. By this approach, the fluorescence spectrum can be calculated using the methods usually applied to obtain the absorption spectrum in the ground state conformation. Although the excited state geometry is not perfectly reproduced, the resulting FF conformation gave a wavelength for the lowest dipole allowed excitation energy, λ_{max}, quite close to that of the excited state, as shown in Scheme 1. The series of nanotubes chosen for the present theoretical study have diameters varying from 7.5 to 10.5 Å. These cylinders can accommodate up to three PFO chains aligned along the nanotube axis. We also considered the possibility that groups of three PFO chains wrap around the tubes forming helices, as illustrated in Figure 1. Differently from previous studies,[3] we found helical arrangements in which the conjugated polymer backbone faces the tube wall. One of the octyl chains also wraps around the tubes while the other points toward the solvent. Typical geometries are shown in Figure 1.

The comparison between aligned and helical wrapping of PFO in SWNT was performed by calculating the average potential energy at 300 K and subtracting the total potential energy of the respective configurations in the ground state, resulting in the relative potential energy ΔE. These energies were plotted as a function of SWNT diameter and chiral angle in Figure 2. Error bars are also indicated and represent the average fluctuation from the dynamics trajectories. We note first that the helical wrapping is better in the sense that it allows a closer contact among the different parts, namely, alkyl−alkyl, alkyl−nanotube, and fluorene−nanotube interactions. As the formation of these PFO helices do not involve large torsion angles between fluorene units, the average energy increase due to torsions is compensated by the attractive interactions. Basically, the helical wrapping has much lower potential energy because it allows the zipping of the
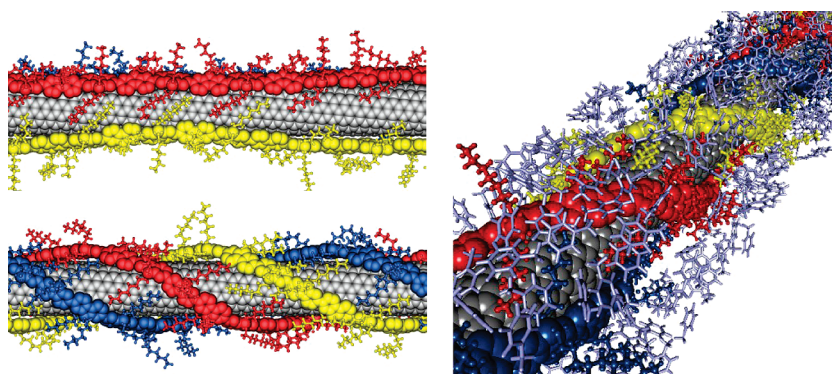
Figure 1. (8,6) Nanotube wrapped by three PFO chains (represented as blue, red, and yellow structures) in two geometries: chains aligned to the tube axis (top, left) and forming helices (bottom, left). The solvated system included enough toluene molecules (light gray structures) to cover the octyl side chains (right).
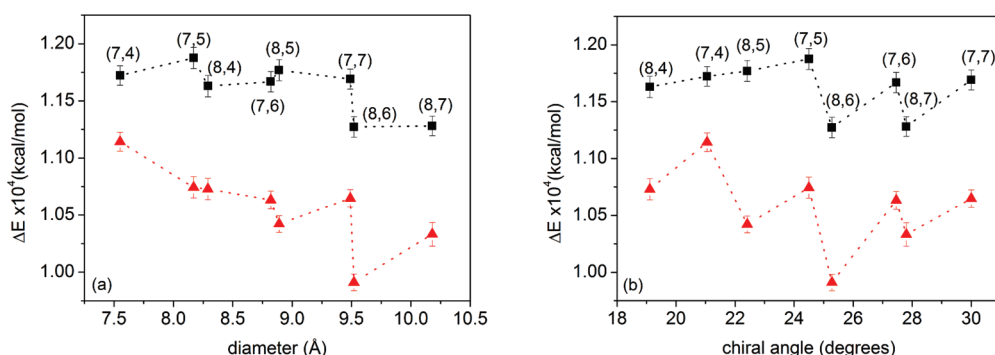

Figure 2. $\Delta E = (E(300\ \text{K}) - E(0))$ for the PFO—SWNT hybrids in toluene, for chains aligned to the tube axis (black) and rolling up as helices (red) as a function of (a) diameter and (b) chiral angle.

alkyl tails regardless of the tube diameter or chirality. Notice in Figure 1 that the wrapping geometry corresponding to chains aligned along the nanotube axis in (8,6) SWNT cannot perfectly attach through octyl—octyl contacts due to the relative sizes of alkyl tail and nanotube diameter. Given the 3-fold zipped chains, the torsions have to be adjusted on each tubule to accommodate the helix that allows the best contacts among the parts. The arrangement obviously depends on nanotube diameter and, more importantly, on chirality. There is a combination involving a diameter and a chiral angle that allows the best interaction contacts, which is represented by the (8,6) nanotube, as evidenced in Figure 2. We also note that, in the wrapping configurations having chains aligned to the nanotube axis, the tubes (8,6) and (8,7) have the lowest potential energies, however, larger than in the helical geometry. We also performed similar MD simulations without toluene and the energy difference between these wrapping schemes is smaller, but still the helical wrapping is more stable. Toluene, thus, seems to favor the helical wrapping.

To test the influence of the underlying β-phase of PFO in toluene on the wrapping process we prepared two sets of experiments in which (i) the solutions are prepared at room temperature and (ii) the PFO solution is first heated at 80 °C for less than 1 min to destroy the chains aggregation, which is seen in the insets of Figure 3 by the vanishing of the characteristic β-phase absorption peak at ~440 nm, and then the nanotubes are added. PFO from Sigma-Aldrich was used in all the experiments for SWNT dispersion. The results are shown in Figure 3. There is a clear enhancement of (8,6) nanotube selectivity upon removal of the aggregated phase of the polymer before the wrapping. This indicates that nanotubes must be working as a template to reform the polymer aggregates.

Another important piece of information comes from the photoluminescence of the polymer wrapping on (7,5) and (8,6) nanotubes. According to the theoretical results, we should expect the PFO chains to be better accommodated on the (8,6) nanotube and thus having a photoluminescence spectrum closer to that of PFO in toluene. Owing to the helix formation in the small diameter (7,5) nanotube we should find differences related to the more stressed polymer structure. Experiments were carried out to measure the fluorescence of the PFO-nanotube hybrids in polymer-free solutions. It is very challenging to really isolate a single PFO-SWNT type; however, given the relative intensities, the luminescence of samples prepared with HiPCO nanotubes should be dominated by the (8,6) tube while in the CoMoCAT samples the (7,5) nanotube has the strongest luminescence intensity.
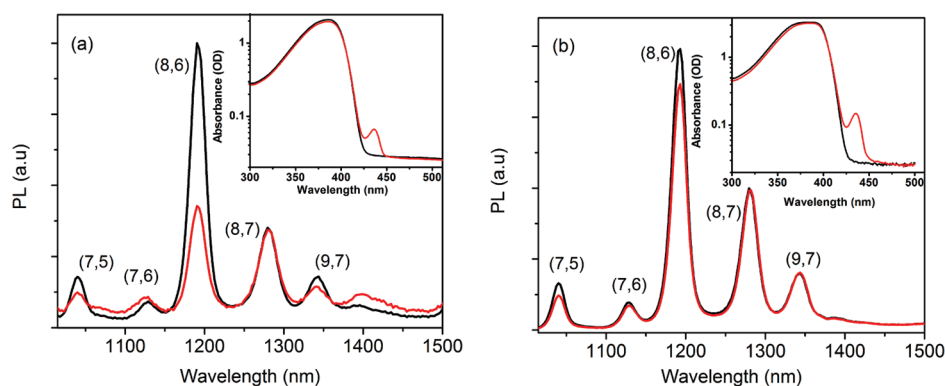
Figure 3. PL spectra of dispersed H-SWNTs in PFO solutions with (black) or without (red) heat treatment in toluene at concentrations of 0.1 mg/mL (a) and 0.2 mg/mL (b). The PL spectra of dispersed nanotubes are normalized at the maximum intensity of the (8,7) tubes. Absorption spectra of PFO solutions are shown in the insets.
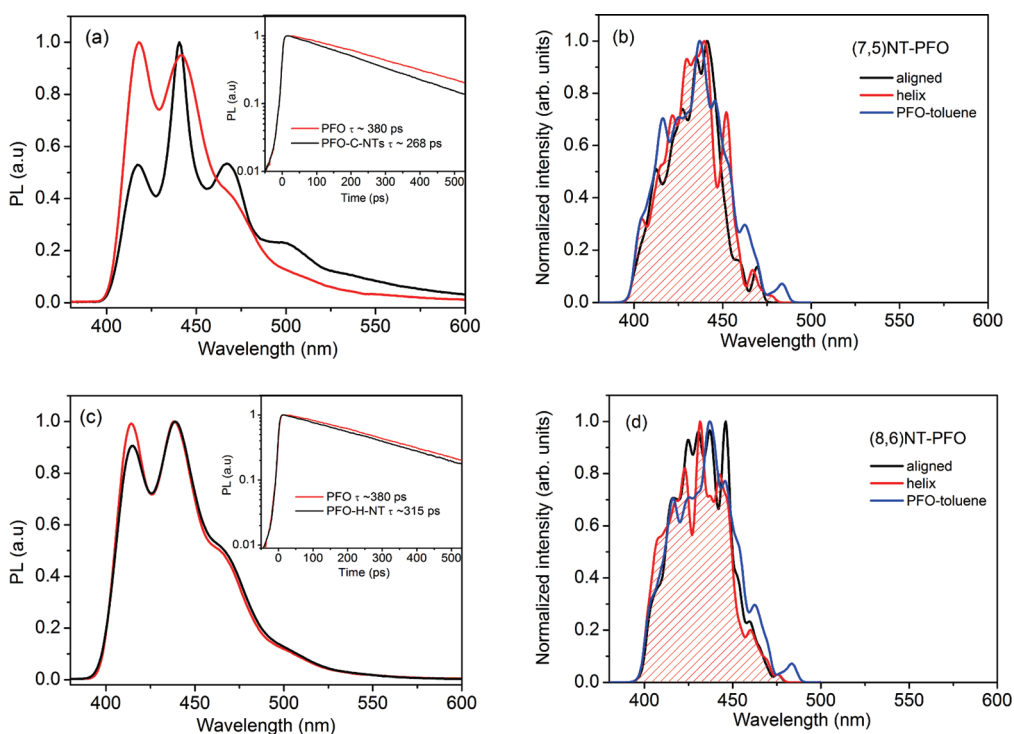
Figure 4. Steady-state and time-resolved (inset) photoluminescence of the PFO (black curves) interacting with CoMoCAT (a) or HiPCO SWNTs (c) after removal of the residual polymer. Red curves are for PFO in toluene. Simulated emission spectra of PFO structures: chains from PFO-(7,5) nanotube (b) and PFO-(8,6) nanotube (d). Black curves are for chains aligned on nanotube axis, red curves are for helical wrapping and blue curves are for free PFO in toluene.

The experimental results are shown in Figure 4, together with the simulated spectra. Figure 4a shows the PL intensity as a function of photon wavelength emission of the PFO-(7,5) nanotube hybrid compared to the PFO solutions in toluene. Although we expect that PFO chains are aggregated in both situations (PFO in solution and PFO attached to the (7,5) nanotube), there is more order in the polymer structure coiled around the nanotube. The alkyl tails that sit on the nanotube are more constrained in their movement, limiting the torsion between fluorene units. The vibronic progression is modified and reflects this new structure. In particular, the feature peaking at 460 nm is enhanced in the PFO−nanotube system. Figure 4b shows our simulated spectra averaged on structures obtained from MD calculations. Three spectra are shown, for the configurations of coiled polymers (red), free polymer chains in solution (blue), and polymers aligned to SWNT axis (black). First we notice that the simulated spectra extend up to 500 nm due to size effects—the simulated chains are much shorter than the actual PFO chains in the experiment. However it is possible to note that polymer chain conformations on the nanotubes are more constrained in their
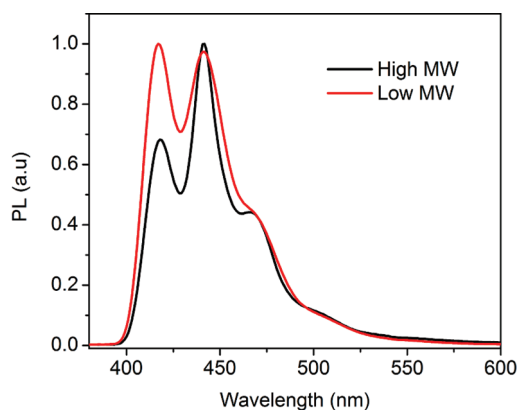
Figure 5. PL spectra of low and high molecular weight PFO samples in toluene.

movements resulting in a sharpened spectrum. A slight decrease of the feature peaking at 410 nm results from it in both the aligned wrapping and helical wrapping configurations. However, the coiled structures present a strong feature peaking at 450 nm which is due to the more stressed polymer structure coiled around a small diameter cylinder. Comparing with the experimental spectra, we conclude that this feature is a signature of the helical wrapping.

Figure 4c and Figure 4d show the experimental PL results and the simulated spectra, respectively, for the PFO-(8,6) hybrid. We notice a much less important modification of the spectrum when compared to the PFO solution, but with a decrease in the intensity of the first peak. In the simulated spectra, the helical conformation gives a three peaks spectrum with a first peak at lower intensity than the second peak, which differs from the aligned wrapping chains in that the peaks have practically all the same intensity. This reflects a more relaxed structure of PFO in the (8,6) nanotube. Although it is less evident that there is a helical wrapping in this case, the comparison with the fluorescence of PFO in toluene from different PFO samples is enlightening. Figure 5 displays the photoluminescence spectra of two diluted PFO samples from different sources, which are labeled as low and high molecular weight (MW). The photoluminescence decays of both samples are monoexponential ($\tau \approx 380$ ps) indicating that single polymer chains are isolated in the solvent. In the low MW sample (MW 58 200) the first and second peaks of the vibronic progression have approximately the same intensity, while other peaks are much weaker. In the high MW samples (MW 40 000−120 000), where chain folding and bending are expected to occur, the vibronic peaks resemble those observed in the PFO-(7,5) nanotube hybrid (Figure 4a). In particular, the first peak corresponding to the (0−0) transition has smaller intensity than the (0−1) transition, which could be interpreted as being a consequence of torsion angles between fluorene units. Torsion angles are needed to form helices as well.

Finally, we discuss the results for the PL decay, shown as insets of Figure 4a and Figure 4c. In both PFO-(7,5) and PFO-(8,6) systems the quenching of the fluorescence was observed indicating that there is an electronic interaction between fluorene units and the nanotubes. However, it is much more pronounced in the PFO-(7,5) nanotube hybrid. Together with the photoluminescence spectra, our data evidence important differences in the polymer conformations wrapping around nanotubes of different diameters and/or chiralities. According to our MD calculations, this is due to a more constrained polymer conformation in the smaller diameter (7,5) nanotube, which involves larger torsion angles between fluorene units.

Very recently, Ozawa et al.[11] demonstrated the recognition/extraction relationship between the copolymer (9,9-bis[n-decyl] fluorene-9,9-bis[(S)-(+)-2-methylbutyl] fluorene) and SWNTs, along with a molecular mechanics modeling. The copolymer selectivity depends on the relative amount of units containing the bulky methylbutyl side group. For copolymers containing more than 80% of those bulky units the polymers wrap preferentially at the (10,3) nanotube, whose chiral angle is 12.7°. The molecular modeling was performed for the binding energy of the hexamer and SWNTs without considering the solvent effect, and the results did not allow for an interpretation of the change in selectivity. Temperature and solvent effects are essential ingredients to properly model these systems, as we showed. Moreover, we explored further our simulations and used the molecular geometries to obtain the fluorescence spectra of the polymers on nanotubes to compare with our experiments.

CONCLUSION

Our results are consistent with a PFO-nanotube interaction in toluene dominated by the octyl−octyl zipping mechanism that locks the polymer chains on the nanotubes, similarly to what has been observed in the β-phase of PFO in toluene. The preference manifested by this polymer to certain nanotubes depends on the tube diameter and chirality: the cylindrical template has to provide an appropriate diameter to the coiling of chains and the carbon−carbon motif of bonds has to be in a proper direction to allow a good contact between octyl chains and the nanotube wall. The fluorene−nanotube interaction plays a smaller role in the polymer adsorption on nanotube walls in the less constrained PFO-(8,6) nanotube system and consequently the modifications of the polymer PL spectrum and decay are less evident. Other studies have also pointed to a preference for helical wrapping of conjugated polymers in SWNT,[12,13] even in the case of conformationally restricted polymer chains.[12] The spontaneous formation of helical patterns of adsorbates on cylinders driven by electrostatic interactions was theoretically demonstrated[14] and extended to

include a competing elastic force.[15] Although our modeling includes more interactions, we believe that our results belong to the same class of phenomena. More importantly, we found that PFO selectivity is strongly dependent on the solvent: it may induce the formation of polymeric supramolecular structures in solution that are transferred to the nanotube walls.

METHODS

Poly(9,9-di-n-octylfluorenyl-2,7-diyl) (PFO) was purchased from Sigma-Aldrich and used as received. These polymers, used to study the polymer−nanotube hybrids, have an average molecular weight (MW) of 58 200. Another PFO sample, purchased from American Dye Source (ADS), has typically much higher molecular weight (MW 40 000−120 000) and was used to evaluate molecular weight effects in absorption and photoluminescence spectra of polymer solutions in toluene. Two kinds of carbon nanotubes, CoMoCAT SWCNT (C-SWNT) from Southwest Nanotech (USA) and HiPCO SWCNT (H-SWNT) from Unidym (USA), were used as received. The C-SWNTs were characterized by a narrower diameter distribution than the H-SWNTs. For the preparation of SWCNT dispersions, 1 mg dry nanotubes were added to 5 mL toluene solution with different polymer concentrations and the mixture was sonicated in a tabletop ultrasonic bath (VWR, The Netherlands). After sonication, the crude dispersion was centrifuged at 5k rpm for 20 min. The supernatant was then removed for further measurements. To wash out the isolated polymer, the solution was filtered through a Teflon membrane filter (100 nm pore size) and rinsed with toluene several times until no photoluminescence (PL) emission was detected from the filtrate. Finally, the filter was steeped in toluene and mildly sonicated for 10 min, yielding a SWNT-enriched solution with minimal polymer residue. Absorption spectra were recorded with a Perkin-Elmer UV−vis−near-infrared spectrophotometer (Lambda 900). Steady-state and time-resolved photoluminescence measurements were performed by exciting the solutions at 760 or 380 nm by a 150 fs pulsed Kerr mode locked Ti:sapphire laser. The steady-state PL of SWCNTs and polymers were measured with InGaAs and Si-CCD detectors, respectively. The time-resolved PL of the dispersion was recorded by Hamamatsu streak cameras working in synchroscan mode. All the measurements were performed at room temperature, and the spectra were calibrated for the instrumental response.

The binding of PFO to (n,m) SWNTs was studied through classical molecular dynamics (MD) in nonperiodic models. Simulations were run in the NVT ensemble at $T = 300$ K, using the Nosé−Hoover thermostat. The solvent toluene was used. Tubes $(7, m)$ and $(8, m)$ $(m = 4,5,6,7)$ were investigated. Structures were built with open ends and have an average length of 200 Å. MD calculations were performed within the Open Force Field module of Cerius 2 package[16] adopting the CVFF950 force field.[17] Forces include bond stretching, bond angle and torsion angle potentials, van der Waals interactions, and Coulomb interactions between atomic charges obtained from density functional calculations. Some force field parameters have been conveniently modified as follows. CVFF attributes atom type "c5" to the sp^2 carbons in a five-membered ring and atom type "c" to the sp^3 carbon bonded to four carbon atoms, such as the one connected to the alkyl chains in PFO. The use of standard CVFF parameters produces a too short B bond in Scheme 1 and the angle centered in the sp^3 carbon involving its two sp^2 neighbors is too acute, compared to the excited state geometry. Thus, our strategy was to widen this angle to increase the B bond and hence get closer to the excited state bond alternation. To accomplish this, a new harmonic term was introduced to this c5−c−c5 angle, with an equilibrium angle at 180° and a force constant of 135.0 kcal/(mol rad^2). To compensate for some distortions induced by this change, the force term for angles of the type c-c5-c5 was stiffened from 120.0 to 145.0 kcal/(mol rad^2) and the Morse potential energy constant between two bonded c5-type atoms was increased

from 70.0 to 110.0 kcal/mol. All other parameters are as in the original CVFF force field.

Snapshots of the conformations from the final 50 ps of MD simulations were used as inputs to calculate the fluorescence spectra of the polymer chains. As a conjugated polymer, polyfluorene has distinct patterns of bond order alternation in the ground and the excited states. To account for that, we calculated the ground state conformation of a fluorene dimer, with methyl replacing octyl side chains, through density functional theory (B3LYP functional[18] with Gaussian 6-31G(d) basis set), also used to attribute net charges on atoms in MD calculations, and the first excited state conformation was obtained by means of a configuration interaction scheme that includes all singly excited Slater determinants (CIS) with the same 6-31G(d) basis set. The excitation spectrum was subsequently calculated using the semiempirical ZINDO/S−CI method.[19] The quantum chemistry package Gaussian 03[20] was used.

A solvent layer was included to cover the wrapped polymer following a procedure previously described.[21] The simulations were run at a time step of 1.5 fs and lasted 500 ps. The selection of polymer conformations at the final 50 ps of simulation took into account the average potential energy and its variation along the simulation. MD snapshots close to the mean potential energy were chosen. A total of 25 snapshots were taken resulting in 75 polymer conformations for each nanotube. The excitation spectra were then calculated through ZINDO/S−CI and averaged. Gaussian lineshapes of 2 nm of half width were used to produce the simulated fluorescence spectra. By this method, each conformation represents a particular snapshot along the vibrational movement of the atoms and thus the vibronic structure of the fluorescence spectrum is captured. A correction was applied to the spectra to smoothly cut off emissions with wavelengths smaller than 400 nm which are actually produced by chain segments closer to the ground state geometry and are part of the absorption spectra.

REFERENCES AND NOTES

1. Saito, R.; Dresselhaus, G.; Dresselhaus, M. S. *Physical Properties of Carbon Nanotubes*; Imperial College Press: London, 1998.
2. Hersam, M. C. Progress Towards Monodisperse Single-Walled Carbon Nanotubes. *Nat. Nanotechnol.* **2008**, *3*, 387–394.
3. Nish, A.; Hwang, J. Y.; Doig, J.; Nicholas, R. J. Highly Selective Dispersion of Single-Walled Carbon Nanotubes Using Aromatic Polymers. *Nat. Nanotechnol.* **2007**, *2*, 640–646.
4. Gao, J.; Loi, M. A. Photophysics of Polymer-Wrapped Single-Walled Carbon Nanotubes. *E. Phys. J. B* **2010**, *75*, 121–126.
5. Kwak, M.; Gao, J.; Prusty, D. K.; Musser, A. J.; Markov, V. A.; Tombos, N.; Stuart, M. C. A.; Browne, W.; Boekema, E. J.; ten Brinke, G.; *et al.* DNA Block Copolymer Doing It All: From Selection to Self-Assembly of Semiconducting Nanotubes. *Angew. Chem., Int. Ed.* **2011**, *50*, 3206–3210.

6. Hwang, J. Y.; Nish, A.; Doig, J.; Douven, S.; Chen, C. W.; Chen, L. C.; Nicholas, R. J. Polymer Structure and Solvent Effects on the Selective Dispersion of Single-Walled Carbon Nanotubes. *J. Am. Chem. Soc.* **2008**, *130*, 3543–3553.

7. Gao, J.; Kwak, M.; Wildeman, J.; Herrmann, A.; Loi, M. A. Effectiveness of Sorting Single-Walled Carbon Nanotubes by Diameter Using Polyfluorene Derivatives. *Carbon* **2011**, *49*, 333–338.

8. Knaapila, M.; Winokur, M. J. Structure and Morphology of Polyfluorenes in Solutions and the Solid State. *Adv. Polym. Sci.* **2008**, *212*, 227–272.

9. O'Carroll, D.; Lieberwirth, I.; Redmond, G. Microcavity Effects and Optically Pumped Lasing in Single Conjugated Polymer Nanowires. *Nat. Nanotechnol.* **2007**, *2*, 180–184.

10. Justino, L. L. G.; Ramos, M. L.; Knaapila, M.; Marques, A. T.; Kudla, C. J.; Scherf, U.; Almasy, L.; Schweins, R.; Burrows, H. D.; Monkman, A. P. Gel Formation and Interpolymer Alkyl Chain Interactions with Poly(9,9-dioctylfluorene-2,7-diyl) (PFO) in Toluene Solution: Results from NMR, SANS, DFT, and Semiempirical Calculations and Their Implications for PFO β -Phase Formation. *Macromolecules* **2011**, *44*, 334–343.

11. Ozawa, H.; Fujigaya, T.; Niidome, Y.; Hotta, N.; Fujiki, M.; Nakashima, N. Rational Concept To Recognize/Extract Single-Walled CarbonNanotubes with a Specific Chirality. *J. Am. Chem. Soc.* **2011**, *133*, 2651–2657.

12. Kang, Y. K.; Lee, O. S.; Deria, P.; Kim, S. H.; Park, T. H.; Bonnell, D. A.; Saven, J. G.; Therien, M. J. Helical Wrapping of Single-Walled Carbon Nanotubes by Water Soluble Poly-(*p*-phenyleneethynylene). *Nano Lett.* **2009**, *9*, 1414–1418.

13. Caddeo, C.; Melis, C.; Colombo, L.; Mattoni, A. Understanding the Helical Wrapping of Poly(3-hexylthiophene) on Carbon Nanotubes. *J. Phys. Chem. C* **2010**, *114*, 21109–21113.

14. Kohlstedt, K. L.; Solis, F. J.; Vernizzi, G.; de la Cruz, M. O. Spontaneous Chirality *via* Long-Range Electrostatic Forces. *Phys. Rev. Lett.* **2007**, *99*, 030602.

15. Solis, F. J.; Vernizzi, G.; de la Cruz, M. O. Electrostatic-Driven Pattern Formation in Fibers, Nanotubes and Pores. *Soft Matter* **2011**, *7*, 1456–1466.

16. *Cerius²*, version 4.10; Accelrys, Inc: SanDiego, CA, 2005.

17. Dauber-Osguthorpe, P.; Roberts, V. A.; Osguthorpe, D. J.; Wolff, J.; Genest, M.; Hagler, A. T. Structure and Energetics of Ligand Binding to Proteins: (*Escherichia coli*) Dihydrofolate Reductase-Trimethoprim, a Drug-Receptor System. *Proteins: Struct., Funct. Genetics* **1988**, *4*, 31–47.

18. Becke, A. D. Density-Functional Thermochemistry: The Role of Exact Exchange. *J. Chem. Phys.* **1993**, *98*, 5648–5652.

19. Zerner, M. C. Semiempirical Molecular Orbital Methods. *Rev. Comput. Chem.* **1991**, *2*, 313–365.

20. Frisch, M. J.; Trucks, G. W.; Schlegel, H. B.; Scuseria, G. E.; Robb, M. A.; Cheeseman, J. R.; Montgomery, J. A., Jr.; Vreven, T.; Kudin, K. N.; Burant, J. C.; *et al. Gaussian 03,* revision E; Gaussian, Inc.: Wallingford, CT, 2004.

21. Carvalho, E. J. F.; dos Santos, M. C. Role of Surfactants in Carbon Nanotubes Density Gradient Separation. *ACS Nano* **2010**, *4*, 765–770.